

Modern Physics Letters A
© World Scientific Publishing Company

Spin alignment measurement of vector mesons produced in high energy collisions

Bedangadas Mohanty

*School of Physical Sciences, National Institute of Science Education and Research, HBNI,
Jatni-752050, India
bedanga@niser.ac.in*

Sourav Kundu

Experimental Physics Department, CERN, CH-1211 Geneva 23, Switzerland

Subhash Singha

*Institute of Modern Physics, Chinese Academy of Sciences Lanzhou,
Gansu 730000, China*

Ranbir Singh

*School of Physical Sciences, National Institute of Science Education and Research, HBNI,
Jatni-752050, India*

Received (Day Month Year)

Revised (Day Month Year)

This review covers the recent experimental development on spin alignment measurements of K^{*0} and ϕ vector mesons in heavy-ion and pp collisions at RHIC and LHC energies. Measurements in e^+e^- collisions at LEP energies are also discussed. Spin alignment of vector mesons are studied by measuring the second diagonal element ρ_{00} of spin density matrix. The spin density matrix element ρ_{00} is obtained by measuring the angular distribution of vector meson decay daughter with respect to the quantization axis in vector meson rest frame. Measured ρ_{00} values for vector mesons are found to be larger than 1/3 at high momentum in e^+e^- collisions at LEP energies, suggesting the preferential production of vector meson with helicity zero state from the fragmentation process. The ρ_{00} values are found to be smaller than 1/3 ($\rho_{00} = 1/3$ implies no spin alignment) for K^{*0} and ϕ vector mesons at low transverse momentum in Pb–Pb collisions at $\sqrt{s_{NN}} = 2.76$ TeV. This observations are qualitatively consistent with the expectation from models which attribute the spin alignment effect due to polarization of quarks in the presence of large initial angular momentum in non-central heavy-ion collisions and its subsequent hadronization by the process of recombination. No significant spin alignment effect is observed for K_S^0 (spin = 0) in mid-central Pb–Pb collisions and for vector mesons in pp collisions. However, the preliminary results of ρ_{00} for ϕ mesons are larger than 1/3 at intermediate p_T in Au–Au collisions at RHIC energies and can be attributed to the presence of ϕ meson field. Although there is evidence of spin alignment effect of vector mesons in heavy-ion collisions but the measured effect is surprisingly larger in context

2 *Bedangadas Mohanty, Sourav Kundu, Subhash Singha and Ranbir Singh*

of hyperon polarization. Therefore these results will trigger further theoretical study.

Keywords: Spin alignment, vector meson. ρ_{00} , heavy-ion

PACS Nos.: include PACS Nos

1. Introduction

The spin-orbital angular momentum interactions are one of the most important effect in nuclear, atomic and condensed matter physics. This causes fine structure and shell structure in atomic and nuclear physics, respectively and is a key ingredient in the field of spintronics in material sciences. The spin-orbital angular momentum interaction is also expected to affect the evolution of hot and dense quark-gluon plasma (QGP), produced in ultra-relativistic heavy-ion collisions. High energy heavy-ion collisions create a temperature more than 10^{13} K at RHIC and 10^{16} K at LHC energies. Under this extreme condition quarks and gluons inside protons and neutrons are set free over an extended volume and leads to the formation of QGP. Heavy-ion collisions offer an ideal environment for studying the properties of QGP phase and test various phenomenon of quantum chromodynamics (QCD).¹

Given the importance of spin-orbit interactions in several fields of physics, it is imperative to look for its possible effect on particles with non-zero spin in a system with high orbital angular momentum. In non-central heavy-ion collisions, where the impact parameter (b) between two colliding nuclei is non-zero, a very large orbital angular momentum (OAM) of the order of $10^5 - 10^7 \hbar$ is expected to be created about the centroid of the participant matter.² In presence of such large OAM, spin-orbit coupling of QCD could lead to the polarization of quarks and anti-quarks in the produced QGP medium. The polarization of quarks and anti-quarks are further translated to the polarization of produced particles with non-zero spin along the direction of the OAM during the process of hadronization.³⁻⁵ The transfer of OAM to the QGP medium in the form of preferential alignment of the spin of the produced particles along the OAM direction is known as global polarization. Statistical mechanics, kinetic theory and hydrodynamics further show that the OAM can be manifested in the form of fluid vorticity.⁶⁻⁹

There are two kinds of polarization of produced hadrons which have been studied in experiment: 1) vector polarization and 2) tensor polarization. The vector polarization has been studied by measuring the polarization of hyperons, whereas the tensor polarization is studied by measuring the polarization of vector mesons. Unlike the polarization of hyperons, which undergo weak decay with parity violation, the polarization of vector meson can not be measured directly as they mainly decay through the parity conserving strong decay. However, the spin alignment of vector mesons can be studied by measuring the diagonal elements of 3×3 hermitian spin density matrix with unit trace. The diagonal elements ρ_{11} , ρ_{00} and ρ_{-1-1} are the probabilities of the spin component of vector mesons along the quantization axis. Among these three diagonal elements, ρ_{00} is independent, whereas ρ_{11} and ρ_{-1-1}

cannot be measured separately in two-body decays to pseudoscalar mesons. Therefore, in experiment, spin alignment of vector mesons has been studied by measuring the ρ_{00} element of the spin density matrix. In the absence of spin alignment, all the three spin states of vector mesons 1, 0 and -1 are equally probable and that makes $\rho_{00} = 1/3$. Any deviation of ρ_{00} from 1/3 is the experimental signature of the spin alignment of the vector mesons. In high energy experiment the diagonal element ρ_{00} is measured from the angular distribution of the vector meson decay daughter with respect to a quantization axis, in vector meson rest frame. Unlike hyperon polarization, spin alignment of vector meson has negligible contamination from the decays as they are predominantly produced directly. For the cases of two body strong decay of vector mesons there is no uncertainty due to the decay parameter as seen for hyperons.

Along with the distinct importance of spin alignment study of vector mesons in heavy-ion collisions, these measurements are also carried out in high energy lepton and hadron collisions in order to understand the production mechanism of vector mesons. In high energy collisions, spin alignment of vector mesons can occur from the fragmentation of un-polarized quarks. Therefore, these measurements are useful to understand the spin dependent fragmentation function and hence considered as one of the important aspects in high energy spin physics.

In this paper, we review the experimental results of the spin alignment of vector mesons in high energy heavy-ion, hadron and lepton collisions. This review is organized as follows: in next section we discuss the experimental observable, followed by a brief description about the coordinate systems used in the experimental analysis. In section 4 we briefly discuss the analysis techniques. In section 5 and section 6 we review the experimental results of spin alignment of vector mesons in e^+e^- and hadron-hadron collisions, and in heavy-ion collisions, respectively. A brief theoretical discussion related to the experimental results are also presented in section 5 and section 6. Finally a summary and future prospects are presented in section 7

2. Experimental observable: angular distribution of vector meson's decay daughter

The spin alignment of vector mesons are studied by measuring the diagonal element ρ_{00} of a 3×3 hermitian spin density matrix.¹⁰ ρ_{00} corresponds to the probability of finding a vector meson in spin state 0 out of 3 possible spin states of -1, 0 and 1. All three states are equally probable in absence of spin alignment. This leads to $\rho_{00} = 1/3$. On the other hand, in the presence of spin alignment ρ_{00} will deviate from 1/3. In experiment, the spin density matrix element ρ_{00} is measured by studying the angular distribution of the decay daughter of vector meson with respect to a quantization axis in vector meson's rest frame. In order to obtain the angular distribution of vector meson decay daughter, let us consider a vector meson is at rest and decays to two spin 0 particles. The projection of the total angular momentum ($\vec{J} = 1$) of vector meson along any arbitrary quantization axis is m . The

4 *Bedangadas Mohanty, Sourav Kundu, Subhash Singha and Ranbir Singh*

completeness relation of vector meson state gives,

$$\sum_{m = -1, 0, 1} |1, m\rangle\langle 1, m| = 1. \quad (1)$$

In the rest frame of vector meson, momentum of two decay daughters are back to back and is denoted as $\vec{p}(\theta^*, \phi^*)$, where θ^* is the polar angle made by vector meson's decay daughter with the quantization axis and ϕ^* is the corresponding azimuthal angle. Using the conservation of final and initial state total angular momentum, two particle final state of decay daughters of vector meson can be expressed in terms of their helicities (λ_1, λ_2) , total angular momentum, polar and azimuthal angle as,

$$|\theta^*, \phi^*, J = 1, \lambda\rangle, \quad (2)$$

where J corresponds to the total angular momentum and the difference between the helicities of two decay daughters is λ . In helicity basis, the final state physically corresponds to a state which have total angular momentum 1 and its projection λ along the flight direction of any one of the decay daughter which is expressed in terms of θ^* and ϕ^* . The λ is given as,

$$\lambda = \lambda_1 - \lambda_2 = (\vec{s}_1 - \vec{s}_2) \cdot \hat{p}, \quad (3)$$

where s_1 and s_2 are the spin of the decay daughters. As the both decay daughters are spin 0 particle, that makes $\lambda = 0$. Therefore the two particle final state of vector meson's decay daughters can be expressed as $|\theta^*, \phi^*, 1, 0\rangle$.

The angular distribution of vector meson decay daughters in the rest frame of vector meson can be expressed as,

$$\frac{dN}{d\cos\theta^*d\phi^*} = \langle \theta^*, \phi^*, 1, 0 | T \rho T^\dagger | \theta^*, \phi^*, 1, 0 \rangle, \quad (4)$$

where T is the transition matrix and ρ is the spin density matrix. By substituting Eq. (1) in Eq. (4), the decay angular distribution can be expressed as,

$$\begin{aligned} \frac{dN}{d\cos\theta^*d\phi^*} &= \sum_m \sum_{m'} \langle \theta^*, \phi^*, 1, 0 | T | 1, M \rangle \\ &\langle 1, m | \rho | 1, m' \rangle \langle 1, m' | T^\dagger | \theta^*, \phi^*, 1, 0 \rangle. \end{aligned} \quad (5)$$

where $\langle \theta^*, \phi^*, 1, 0 | T | 1, m \rangle$ is the transition amplitude of a state $|1, 0\rangle$ from the state $|1, m\rangle$. Using the Wigner D-matrix formalism,¹¹ the decay amplitude is written as,

$$\langle \theta^*, \phi^*, 1, 0 | T | 1, m \rangle = c D_{m, 0}^{1\dagger}(\phi^*, \theta^*, -\phi^*), \quad (6)$$

where D is the Wigner D -matrix element and c is the normalization constant. By substituting Eq. (6) in Eq. (5), we get

$$\frac{dN}{d\cos\theta^*d\phi^*} = \sum_T \sum_{T'} D_{m, 0}^{1\dagger} \rho_{m, m'} D_{m', 0}^1, \quad (7)$$

where $\rho_{m,m'} = \langle 1, m | \rho | 1, m' \rangle$ are the density matrix elements. The Wigner D -matrix elements are given by,

$$D_{1,0}^1 = -\frac{1}{2} \sin \theta^* \exp^{-i\phi^*}, \quad (8)$$

$$D_{0,0}^1 = -\cos \theta^*, \quad (9)$$

$$D_{-1,0}^1 = \frac{1}{2} \sin \theta^* \exp^{i\phi^*}. \quad (10)$$

Using the Wigner D -matrix elements, Eq. (7) can be expressed as,

$$\begin{aligned} \frac{dN}{d \cos \theta^* d\phi^*} \propto & [\cos^2 \theta^* \rho_{00} + \sin^2 \theta^* (\rho_{11} + \rho_{-1-1})/2 \\ & + \sin 2\theta^* \cos \phi^* (\text{Re} \rho_{-10} - \text{Re} \rho_{01})/\sqrt{2} \\ & + \sin 2\theta^* \sin \phi^* (\text{Im} \rho_{-10} - \text{Im} \rho_{01})/\sqrt{2} \\ & - \sin^2 \theta^* (\cos 2\phi^* \text{Re} \rho_{1-1} + \sin 2\phi^* \text{Im} \rho_{-11})] \end{aligned} \quad (11)$$

The unit trace condition of spin density matrix elements $\rho_{-1-1} + \rho_{00} + \rho_{11} = 1$ and integration over azimuthal angle leads Eq. (11) to

$$\frac{dN}{d \cos \theta^*} \propto [1 - \rho_{00} + (3\rho_{00} - 1) \cos^2 \theta^*]. \quad (12)$$

3. Coordinate system

In experiment, three widely used coordinate system for spin alignment measurements are 1) helicity frame, 2) production plane and 3) reaction plane. In helicity frame the quantization axis is the momentum direction of the vector meson in lab frame and θ^* is the angle made by vector meson decay daughter with the quantization axis in vector meson rest frame as shown in the panel (c) of Fig. 1. The panel (b) of Fig. 1 shows the graphical illustration of the production plane. In production plane analysis quantization axis is the perpendicular direction of the production plane which is defined by the beam direction and the momentum direction of the vector meson. The reaction plane is defined by the beam direction and the impact parameter direction, and perpendicular direction to the reaction plane can also be used as a quantization axis as shown in the panel (a) and (d) of Fig. 1 for K^{*0} and ϕ , respectively. The perpendicular direction of the reaction plane also corresponds the direction of the initial global angular momentum. In experiment, we can not measure the impact parameter direction. Therefore, we use the event plane as a proxy of the reaction plane and further correct the measurements with event plane resolution. The event plane is estimated from the azimuthal angle of the produced hadrons and can be expressed in terms of event plane vector as,

$$\vec{Q} = \frac{1}{n} \left[\sum_{i=1}^N \sin n\phi_i \hat{i} + \sum_{i=1}^N \cos n\phi_i \hat{j} \right], \quad (13)$$

6 *Bedangadas Mohanty, Sourav Kundu, Subhash Singha and Ranbir Singh*

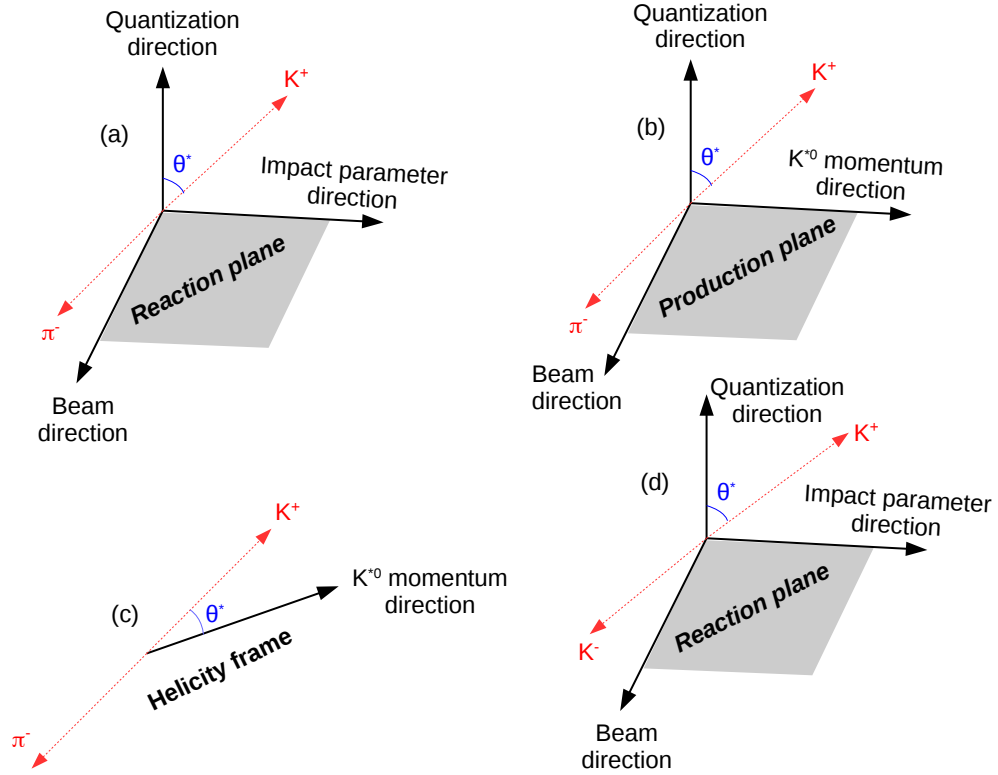


Fig. 1. A graphical illustration of various frame of reference used in spin alignment measurement of vector meson.

where the \vec{Q} is the event plane vector, n is the order of the event plane, summation is over all produced charged particle and ϕ_i is the azimuthal angle of the i^{th} charged particle. In order to derive the relation between measured ρ_{00} w.r.t. the event plane and the reaction plane, let us assume a right handed coordinate system with the impact parameter direction, the beam direction and the angular momentum direction are along x , z and y axis, respectively. The reaction plane is represented by the xz plane. In the rest frame of vector meson the unit momentum vector (\hat{p}) of one of its decay daughter makes the polar angle θ^* and the azimuthal angle ϕ^* . Let us consider the event plane vector is along x' and can be obtained by a rotation of angle ψ about the z axis. Figure 2 shows the reaction plane coordinate system along with the event plane vector. The distribution of the event plane vector is centered around the x with finite resolution. The event plane resolution (R) can be estimated by averaging ψ over a large number of events. The distribution of ψ over many events is an even function centered at zero that gives

$$R = \langle \cos(2\psi) \rangle, \text{ and } \langle \sin(2\psi) \rangle = 0. \quad (14)$$

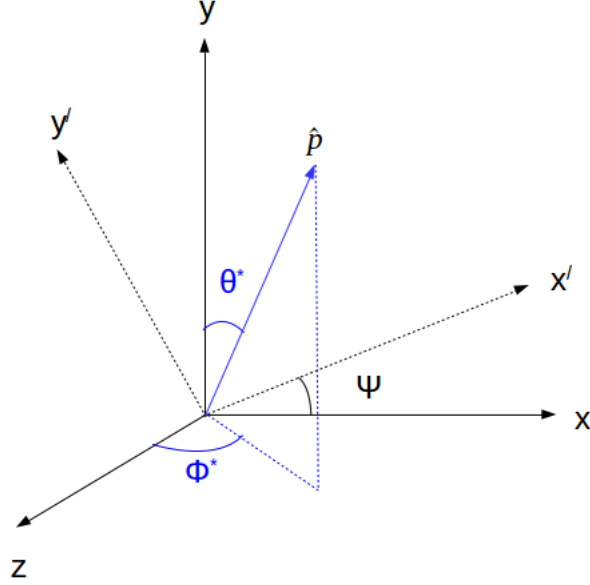


Fig. 2. The reaction plane coordinate system along with the event plane vector obtained by rotating xy plane by angle ψ with respect to z axis.

The angular distribution of decay daughter of vector meson with respect to the quantization axis perpendicular to the reaction plane can be expressed as,

$$\begin{aligned} \frac{dN}{d\cos\theta^*d\phi^*} \propto & [\cos^2\theta^*\rho_{00}^{\text{RP}} + \sin^2\theta^*(\rho_{11}^{\text{RP}} + \rho_{-1-1})/2 \\ & + \sin 2\theta^*\cos\phi^*(\text{Re}\rho_{-10}^{\text{RP}} - \text{Re}\rho_{01}^{\text{RP}})/\sqrt{2} \\ & + \sin 2\theta^*\sin\phi^*(\text{Im}\rho_{-10}^{\text{RP}} - \text{Im}\rho_{01}^{\text{RP}})/\sqrt{2} \\ & - \sin^2\theta^*(\cos 2\phi^*\text{Re}\rho_{1-1}^{\text{RP}} + \sin 2\phi^*\text{Im}\rho_{-11}^{\text{RP}})] \end{aligned} \quad (15)$$

The unit vectors in the reaction plane frame and in the event plane frame are related by,

$$\hat{x} = \cos(\psi)\hat{x}' - \sin(\psi)\hat{y}', \quad (16)$$

$$\hat{y} = \sin(\psi)\hat{x}' + \cos(\psi)\hat{y}', \quad (17)$$

and

$$\hat{z} = \hat{z}'. \quad (18)$$

Let us consider in event plane frame, the polar and azimuthal angles are θ' and ϕ' . The momentum direction of vector meson's decay daughter in two different frames

8 *Bedangadas Mohanty, Sourav Kundu, Subhash Singha and Ranbir Singh*

can be expressed as,

$$\begin{aligned}\hat{p} &= \sin\theta^* \cos\phi^* \hat{z} + \sin\theta^* \sin\phi^* \hat{x} + \cos\theta^* \hat{y} \\ &= \sin\theta^{*'} \cos\phi^{*'} \hat{z}' + \sin\theta^{*'} \sin\phi^{*'} \hat{x}' + \cos\theta^{*'} \hat{y}'.\end{aligned}\quad (19)$$

By substituting Eq. (16), (17) and (18) in Eq. (19) we get,

$$\hat{p} \cdot \hat{z} = \sin\theta^* \cos\phi^* = \sin\theta^{*'} \cos\phi^{*'}.\quad (20)$$

$$\hat{p} \cdot \hat{x} = \sin\theta^* \sin\phi^* = \sin\theta^{*'} \sin\phi^{*'} \cos\psi - \cos\theta^{*'} \sin\psi.\quad (21)$$

$$\hat{p} \cdot \hat{y} = \cos\theta^* = \sin\theta^{*'} \sin\phi^{*'} \sin\psi + \cos\theta^{*'} \cos\psi.\quad (22)$$

By substituting Eq. (20), Eq. (21) and Eq. (22) in Eq. (15) and after integrating over $\phi^{*'}$ we get,

$$\begin{aligned}\frac{dN}{d\cos\theta^{*'}} &\propto \left[1 - \{\rho_{00}^{\text{RP}} - \frac{1}{2} \sin^2\psi(3\rho_{00}^{\text{RP}} - 1)\} \right] \\ &+ \left[3\{\rho_{00}^{\text{RP}} - \frac{1}{2} \sin^2\psi(3\rho_{00}^{\text{RP}} - 1)\} - 1 \right] \cos^2\theta^{*'} \\ &\propto (1 - \rho_{00}^{\text{EP}}) + (3\rho_{00}^{\text{EP}} - 1) \cos^2\theta^{*'}.\end{aligned}\quad (23)$$

From Eq. (23), the relation between ρ_{00}^{RP} and ρ_{00}^{EP} can be written as,

$$\rho_{00}^{\text{EP}} = \rho_{00}^{\text{RP}} - \frac{1}{2} \sin^2\psi(3\rho_{00}^{\text{RP}} - 1).\quad (24)$$

Event average of Eq. 24 gives,

$$\rho_{00}^{\text{RP}} - \frac{1}{3} = \left(\rho_{00}^{\text{EP}} - \frac{1}{3} \right) \frac{4}{1 + 3R}.\quad (25)$$

4. Analysis technique

K^{*0} and ϕ are short lived resonance particles and can not be detected directly in detector. Therefore, K^{*0} and ϕ vector mesons are reconstructed from the invariant mass distribution of oppositely charged daughter pairs ($K^{*0} (\bar{K}^{*0}) \rightarrow K^+(K^-)\pi^-(\pi^+)$) and $\phi \rightarrow K^+K^-$). Charged decay daughters are identified with various particle identification techniques, depending upon the detector configuration. Two such particle identification techniques used in the ALICE and the STAR experiments are: the specific energy loss measured in the Time Projection Chamber (TPC) and the velocity measured by the Time-Of-Flight (TOF) detector. The invariant mass distribution of resonance decay daughters consists of resonance signal and a large combinatorial background. The combinatorial background can be estimated by different techniques such as mixed event background, like sign background and rotational background. After the combinatorial background subtraction resonance signal is visible on top of a residual background, which comes due to the production of correlated daughter pairs from the decays of other hadrons and from

jets. Resonance signal along with the residual background are fitted with combination of a signal fit function and a background fit function. The Breit-Wigner (Voigtian) distribution function is widely used to describes the K^{*0} (ϕ) signal, whereas a second order polynomial is used to describe the residual background. Vector mesons signals are extracted in various $\cos\theta^*$ bins and are corrected for the detector acceptance \times efficiency to get the corrected yields. A Monte Carlo simulation of the detector response based on a GEANT simulation is used to determine the acceptance \times efficiency. The acceptance and efficiency corrected $\cos\theta^*$ distributions are fitted with Eq. (12) to extract ρ_{00} values for vector mesons. Details about the analysis techniques can be found in.^{12,13} An alternative analytic approach for correcting the acceptance effects in ρ_{00} measurement is proposed in.¹⁴

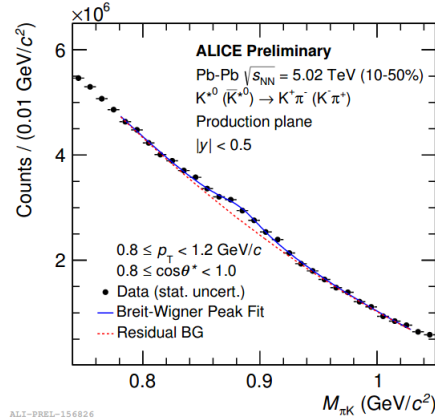


Fig. 3. Mixed event background subtracted invariant mass distribution of unlike charged $K\pi$ pairs in Pb–Pb collisions at $\sqrt{s_{NN}} = 2.76$ TeV, fitted with a Breit-Wigner function + 2nd order polynomial function in $M_{K\pi}$. This distribution is obtained for $0.8 < p_T < 1.2$ GeV/c and $0.8 < \cos\theta^* < 1.0$, and the quantization axis is along the perpendicular direction to the event plane. This figure is taken from ¹⁵

Figure 3 shows a typical invariant mass distribution of unlike charge $K\pi$ pairs after mixed event combinatorial background subtraction in Pb–Pb collisions as a representative plot for K^{*0} signal extraction. The invariant mass distribution is fitted with combination of a Breit-Wigner and a second order polynomial function. Area under the Breit-Wigner distribution is the measured K^{*0} yield in a given p_T and $\cos\theta^*$ interval. The acceptance \times efficiency corrected K^{*0} and ϕ meson

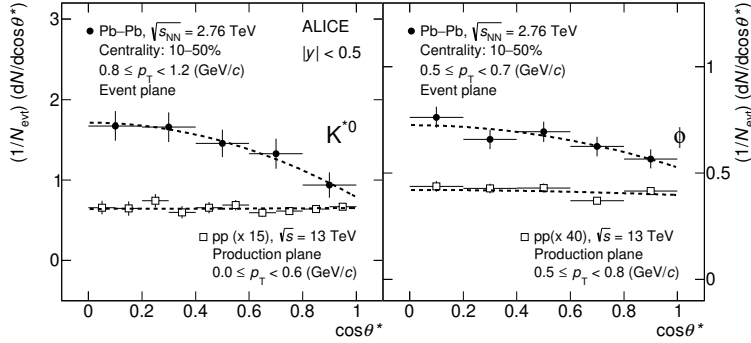


Fig. 4. Acceptance and efficiency corrected angular distribution of the decay daughter of K^{*0} and ϕ vector mesons in Pb–Pb collisions at $\sqrt{s_{NN}} = 2.76$ TeV and in pp collisions at $\sqrt{s} = 13$ TeV. Measurements are carried out in $|y| < 0.5$. Each distribution is fitted with Eq. (12) to obtain ρ_{00} value. Statistical uncertainty on data points are represented by the vertical line.

yield as a function of $\cos \theta^*$ for selected p_T intervals in pp collisions at $\sqrt{s} = 13$ TeV and in mid-central Pb–Pb collisions at $\sqrt{s_{NN}} = 2.76$ TeV are shown in Fig. 4. These distributions are fitted with Eq. (12) to obtain ρ_{00} values. The angular distributions for K^{*0} and ϕ vector mesons in Pb–Pb collisions at $\sqrt{s_{NN}} = 2.76$ TeV with respect to the normal of the event plane and in pp collision at $\sqrt{s} = 13$ TeV with respect to the normal of the production plane are shown in Fig. 4.

5. Spin alignment measurements in small collision system

Spin alignment measurements of light flavour vector mesons have been carried out in helicity frame for e^+e^- collisions, in order to understand the vector meson production mechanism. There are several models of vector meson production which predict the ρ_{00} values in the helicity frame. Spin counting based statistical model^{16,17} assume that the fragmentation process produces extra quark–antiquark pairs with all helicity states being equally probable. In this model framework, a vector meson with helicity $\lambda = \pm 1$ will be produced if the spin of primary and secondary quarks are in parallel. If the spin of primary and secondary quarks are in antiparallel, then either a vector meson or a pseudo-scalar meson could be produced with probability $1 - f$ and f . This production mechanism of vector meson leads to a ρ_{00} value of $\frac{1-f}{1-2f}$ which ranges between 0 to 0.5. In terms of the ratio of pseudoscalar to vector meson production ration (P/V) the ρ_{00} can also be expressed as $\rho_{00} = \frac{1}{2} (1 - (P/V))$. The QCD-inspired model, discussed in¹⁸ describe the fragmentation of soft gluons which are emitted from the fast primary quark. Soft gluons are fragmented into quark-antiquark pairs and at the end of the fragmentation chain the soft antiquark combine with the fast quark of same helicity to produce a vector meson. In this model framework produced vector mesons have $\rho_{00} = 0$. On the other hand, QCD based model described in¹⁶ predicts the production of of vector mesons with $\lambda = 0$. In this model framework vector mesons are produced through the channel $q \rightarrow qV$

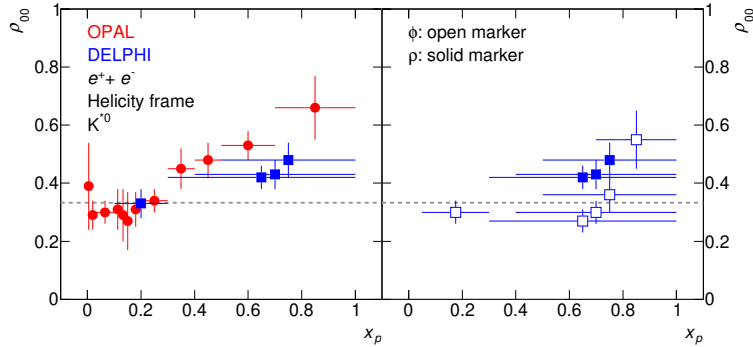


Fig. 5. Spin density matrix element ρ_{00} as a function of x_p for K^{*0} , ϕ and ρ meson in e^+e^- collisions.^{25–27} Measurements were carried out in the helicity frame. Uncertainties on data points are the quadrature sum of statistical and systematics uncertainties.

and the coupling of vector meson with quark is like a vector current coupling. In such case, helicity conservation of vector current ensures the vector meson production with $\lambda = 0$ which corresponds to $\rho_{00} = 1$. Similar prediction for ρ_{00} has also been predicted by other QCD based model^{19–21} in which the hadron energy is equally shared by constituent quarks.

The OPAL^{25,26} and DELPHI experiments²⁷ have measured the spin density matrix element ρ_{00} in helicity frame. The ρ_{00} is larger than $1/3$ for light flavour vector mesons K^{*0} , ϕ and ρ in high x_p ($\frac{p}{p_{beam}}$) region, whereas at low x_p the measurements are consistent with $1/3$. Measurements of ρ_{00} for ρ , K^{*0} and ϕ mesons, measured by DELPHI and OPAL collaboration are shown in Fig. 5. Measured ρ_{00} values for K^{*0} and ρ vector mesons are larger than $1/3$ for $x_p > 0.3$, whereas DELPHI collaboration have observed $\rho_{00} > 1/3$ for ϕ meson for $x_p > 0.7$. Measurements from DELPHI collaboration are further confirmed by OPAL collaboration,²⁶ where they have also observed $\rho_{00} > 1/3$ for ϕ meson for x_E (E/E_{lab}) > 0.7 . This observation rules out the spin counting based statistical model^{16,17} which gives the maximum ρ_{00} value of 0.5. However this can only happen when the probability of production of pseudo-scalar mesons containing the primary quark is zero. Observed spin alignment of vector mesons by DELPHI and OPAL collaboration indicates the preferential production of vector meson in helicity zero state. This observation is consistent with the QCD based vector meson production mechanism, discussed in.^{16,19–21} The OPAL and DELPHI experiments have also measured the off diagonal matrix element ρ_{1-1} and they are found to be consistent with zero, ruling out the models^{22–24} which predict non-zero off-diagonal elements due to coherence phenomena. Within present uncertainties, no evidence has been observed for such effects.

Spin density matrix element ρ_{00} for K^{*0} and K^{*+} have also been studied in kp and nC interaction^{28–32} with respect to the direction the perpendicular to production plane. The ρ_{00} values in these measurements are found to be significantly

higher than the $1/3$ which can be explained by a parton recombination model³⁴ and attributes the spin alignment of vector mesons via Thomas precession of the quark's spin in the recombination process of hadronization. Spin alignment measurements for K^{*0} and ϕ vector mesons with respect to the production plane have been also carried out in high energy pp collisions at the RHIC and the LHC. Figure 6 shows the measured ρ_{00} values for K^{*0} and ϕ vector mesons in pp collisions at $\sqrt{s} = 200$ GeV³⁵ and 13 TeV.¹² Measured ρ_{00} values are consistent with $1/3$ in the studied p_T region for K^{*0} and ϕ vector mesons at both RHIC and LHC energies. However,

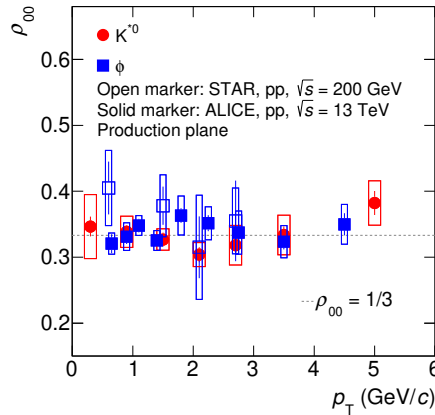


Fig. 6. Spin density matrix element ρ_{00} as a function of p_T for K^{*0} and ϕ vector mesons in pp collisions at $\sqrt{s} = 200$ GeV³⁵ and 13 TeV.¹² Measurements were carried out in the production frame. Statistical and systematic uncertainties on data points are represented by bars and boxes, respectively.

recent theoretical study in³⁶ has predicted a significant spin alignment of vector mesons with respect to helicity frame in high energy pp collisions in fragmentation region (high p_T or high $x_F = 2p_z/\sqrt{s}$). In QCD, the spin alignment of vector meson produced in high energy reactions is determined by the spin-dependent fragmentation function D_{1LL} . In Ref.³⁶ authors have used the measured ρ_{00} values for K^{*0} from e^+e^- collisions and estimated the ρ_{00} values for vector mesons in high energy pp collisions. They have found a significant spin alignment for K^{*0} and ρ vector mesons at high x_F and high p_T as shown in Fig. 7 and Fig. 8. This theory prediction can be further tested in RHIC and LHC energies to understand the vector meson production mechanism at fragmentation region.

6. Spin alignment measurements in heavy-ion collisions

Spin alignment measurements have been recently carried out in heavy-ion collisions at RHIC and LHC energies in order to understand the spin-orbital angular momentum interaction. A large initial angular momentum and magnetic field is expected

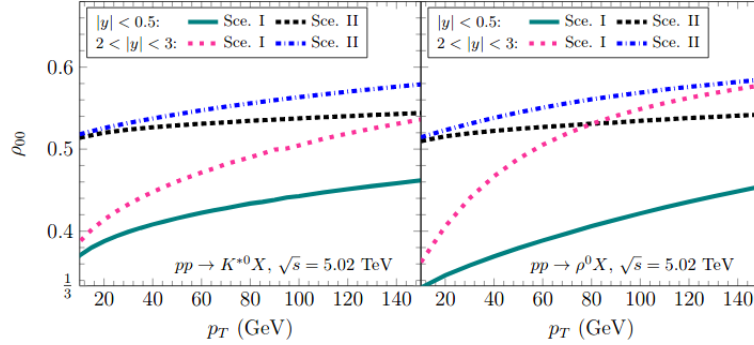


Fig. 7. Spin alignments of K^{*0} and ρ vector mesons in pp collisions at LHC energy $\sqrt{s} = 5.02$ TeV in two rapidity regions as functions of p_T . The figure is taken from.³⁶

to be created perpendicular to the reaction plane in the initial stages of non-central (impact parameter $\sim 3\text{--}10$ fm) heavy-ion collisions. The magnetic field is expected to be short-lived (a few fm/c), whereas the angular momentum is conserved, and its effect could present throughout the evolution of the system formed in the collision. In the presence of a large initial angular momentum produced quarks can be polarized due to the spin-orbital angular momentum interaction of QCD which further leads to the net polarization of vector mesons (K^{*0} and ϕ).^{3-5,37,38} Spin alignment measurement of vector mesons provide a unique opportunity to probe these initial conditions of heavy-ion collisions and can shed light on the presence of spin-orbital angular momentum interaction in heavy-ion collisions.

In theory there are some specific predictions from quark model for vector meson spin alignment and hydrodynamical calculation. In the the presence of a large angular momentum, the spin-orbit coupling of QCD could lead to a polarization of quarks followed by a net-polarization of vector mesons along the direction of the angular momentum.^{3-5,38} Quark model predicts^{3-5,38} $\rho_{00} < 1/3$ if the vector meson is produced from the recombination of two polarized quarks. The recombination hadronization scenario polarized quark is expected to be observed at low p_T and in mid-rapidity. On the other hand quark polarization model predicts $\rho_{00} > 1/3$ if the hadronization of a polarized quarks proceeds via the fragmentation process. Fragmentation hadronization scenario is expected to be observed at high p_T and in forward rapidity. In quark polarization model, polarization of quark is inversely pro-

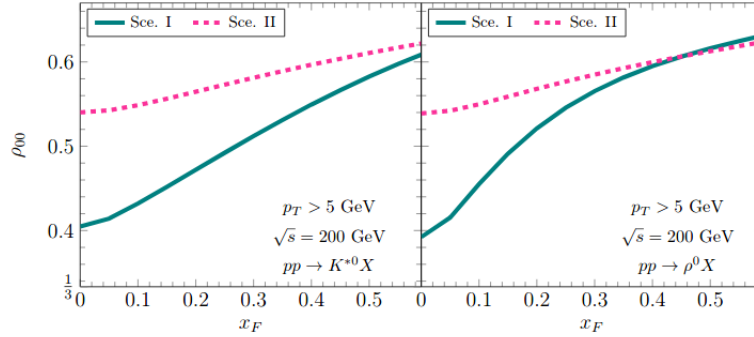


Fig. 8. Spin alignments of K^{*0} and ρ vector mesons in pp collisions at RHIC energy $\sqrt{s} = 200$ GeV in two rapidity regions as functions of x_F . The figure is taken from.³⁶

portional to square of its mass which suggests the spin alignment effect is larger for K^{*0} than ϕ due to their constituent quark composition. Recent theory calculation in³⁹ predicts the existence of coherence ϕ meson field as a source of spin alignment of ϕ meson which leads to $\rho_{00} > 1/3$ for the ϕ meson. In quark model scenario, the initial large magnetic field may also affect the ρ_{00} .³⁸ For neutral vector mesons the magnetic field leads to $\rho_{00} > 1/3$, and for charged vector mesons it leads to $\rho_{00} < 1/3$. On the other hand, recent hydro-dynamical calculation⁴⁰ predicts $\rho_{00} < 1/3$.

Figure 9 shows ρ_{00} values as a function of p_T for K^{*0} and ϕ vector mesons, and K_S^0 meson at $|y| < 0.5$ in Pb–Pb collisions at $\sqrt{s_{NN}} = 2.76$ TeV¹² with respect to the normal to the event plane. Measured ρ_{00} values for the K^{*0} and ϕ with respect to the event plane (EP) in 10–50% Pb–Pb collisions at $\sqrt{s_{NN}} = 2.76$ TeV deviate from $1/3$ at low p_T , whereas at high p_T , measurements are consistent with $1/3$. For spin 0 hadron K_S^0 in 20–40% Pb–Pb collisions measured ρ_{00} values are consistent with $1/3$ throughout the whole measured p_T interval as expected. Measured ρ_{00} values for vector mesons are consistent with $1/3$ in control measurements such as pp collisions where the initial angular momentum is not expected. ALICE collaboration has also performed the spin alignment studies with respect to a quantization axis which is random in 3 dimension and the measured ρ_{00} values are consistent with $1/3$ as expected.¹²

ALICE collaboration has also measured the spin density matrix element ρ_{00} for vector mesons with respect to the normal direction of the production plane and the

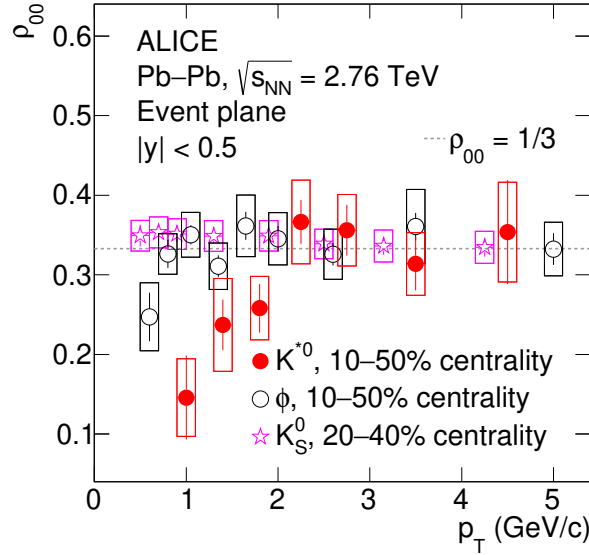


Fig. 9. The p_T dependence of ρ_{00} values for K^{*0} , ϕ , and K_S^0 mesons at $|y| < 0.5$ in mid-central Pb-Pb collisions at $\sqrt{s_{NN}} = 2.76$ TeV.¹² The statistical and systematic uncertainties are shown as bars and boxes, respectively.

random event plane and these measurements are related to the measurements with respect to the normal direction of the event plane. The relation between measured ρ_{00} with respect to two different frames of references is

$$\rho_{00} (A) - \frac{1}{3} = \left(\rho_{00} (B) - \frac{1}{3} \right) \left(\frac{1}{4} + \frac{3}{4} \cos 2\psi \right), \quad (26)$$

where frame A is obtained by rotating frame B by angle ψ . Averaging over angle ψ gives,

$$\rho_{00} (A) - \frac{1}{3} = \left(\rho_{00} (B) - \frac{1}{3} \right) \left(\frac{1}{4} + \frac{3}{4} \langle \cos 2\psi \rangle \right). \quad (27)$$

The transformation from the event plane (EP) to production plane (PP) is obtained by taking into account the elliptic flow of the vector meson which leads to

$$\langle \cos 2\psi \rangle = \frac{1}{2\pi} \int_{-\pi}^{\pi} \cos(2\psi) [1 + 2v_2 \cos(2\psi)] d\psi = v_2. \quad (28)$$

Using Eq. 27 and Eq. 28, analytical relation between EP and PP can be expressed as,

$$\rho_{00} (PP) - \frac{1}{3} = \left(\rho_{00} (EP) - \frac{1}{3} \right) \left(\frac{1 + 3v_2}{4} \right). \quad (29)$$

In order to verify 29 a toy model simulation with PYTHIA (version 8.2) event generator⁴¹ is carried out. PYTHIA does not have any azimuthal anisotropy and

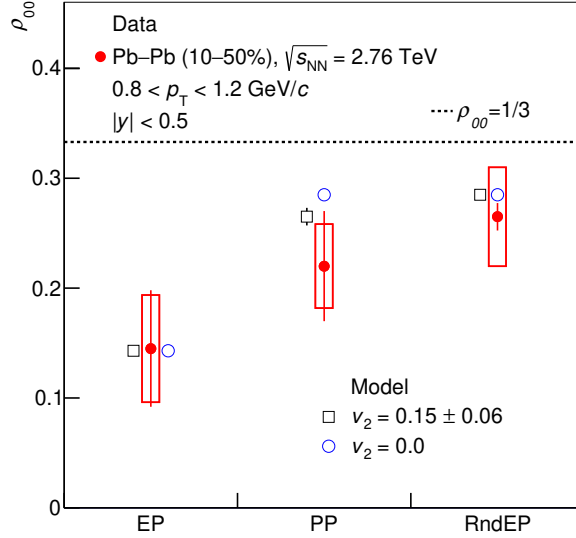


Fig. 10. ρ_{00} values from data in 10–50% Pb–Pb collisions at $0.8 < p_T < 1.2$ GeV/ c with respect to various planes¹² compared with expectations from model simulations with and without added elliptic flow (v_2). The statistical and systematic uncertainties are shown as bars and boxes, respectively. This figure has been taken from.¹²

spin alignment. For this study we have taken event plane angle as zero, which corresponds impact parameter along x -axis. In order to find the relations between different frames, v_2 (0.15 ± 0.06 , value expected for hadrons with mass similar to K^{*0} in Pb–Pb collisions at $\sqrt{s_{NN}} = 2.76$ TeV⁴²) is introduced to K^{*0} by appropriate rotation of its momentum in azimuthal plane. The modified angle in azimuthal plane is calculated by solving the following equation

$$\phi_0 = \phi + v_2 \sin 2\phi, \quad (30)$$

where ϕ_0 is azimuthal angle of K^{*0} in absence of v_2 and for a given value of v_2 , ϕ_0 transforms to ϕ . Then spin alignment through ρ_{00} same as measured in data is introduced with respect to event plane by rotating the momentum of decay daughters in K^{*0} rest frame by solving

$$\cos \theta_0^* = 3/2 \times [(1 - \rho_{00}) \cos \theta^* + 1/3(3\rho_{00} - 1) \cos^3 \theta^*]. \quad (31)$$

Here θ_0^* is the angle made by the decay daughter of K^{*0} with the quantization axis in absence of spin alignment. θ_0^* transforms to θ^* to introduce a given input value of ρ_{00} . In this study we assume that the ϕ^* remain fixed during the rotation. With these modifications, calculations as in the experimental data are carried out. The results are shown in Fig. 10 for two cases, with and without v_2 . The result corresponding to event plane is correctly retrieved in the model. The model results

for $v_2 = 0$, are same for production plane and random event plane. However with $v_2 = 0.15$, the ρ_{00} (PP) value is lower and closer to data for PP. The toy model reproduces the hierarchy observed in the ρ_{00} values for various planes as observed in data. RndEP is defined by randomizing the event plane angle in the azimuthal plane (xy plane). The quantization axis is obtained by taking cross product of event plane vector and z-axis (beam axis). Hence, the quantization axis is always in the xy plane, and a residual effect is present due to use of a common z-axis. Decay daughters of polarized vector mesons could have angular correlation with respect to the z-axis. This residual effect is due to the angular distribution of decay daughters, which follow a oblate or prolate shape, which is rotationally symmetric around the quantization axis (when the off-diagonal terms in the spin density matrix are zero). Rotating such a shape around the z-axis does not lead to a uniform decay angular distribution. This effect results in small deviation of ρ_{00} values from $1/3$ for RndEP. This deviation of ρ_{00} from $1/3$ for RndEP has been also discussed in Ref.⁴³ The physical picture is that spin alignment with respect to the event plane is coupled to that in the production plane through the elliptic flow of the system. The ρ_{00} (RndEP) is lower than $1/3$ as the quantization axis is always perpendicular to the beam axis, resulting in a residual effect. This residual effect can be removed by choosing the quantization axis in a random direction in 3 dimensions for each event. If the quantization axis is random in 3 dimension, then the residual effect is not present and the ρ_{00} value is consistent with $1/3$. On the other hand, preliminary spin alignment measurements of ϕ meson at RHIC energies⁴⁴ shows $\rho_{00} > 1/3$ in intermediate p_T (above $1.2 \text{ GeV}/c$) which is in contrast with the ALICE measurement that shows a deviation ($\rho_{00} < 1/3$) at low p_T below $0.7 \text{ GeV}/c$ where the measurements at RHIC energies do not exist till date. Figure 12 shows the comparison of p_T dependence of ρ_{00} for ϕ meson between Pb–Pb and Au–Au collisions at $\sqrt{s_{NN}} = 2.76 \text{ TeV}$ and 200 GeV , respectively.

ALICE collaboration has also observed a clear centrality dependence of spin alignment for K^{*0} and ϕ meson at low p_T .¹² Deviation of ρ_{00} from $1/3$ is maximum at mid central collisions, whereas in central and peripheral collisions ρ_{00} values are consistent or closed to $1/3$. The observed centrality dependence of spin alignment for K^{*0} and ϕ vector mesons are consistent with the impact parameter dependence of initial angular momentum. Figure 11 shows comparison of p_T and centrality dependence of ρ_{00} for K^{*0} in Pb–Pb collisions at $\sqrt{s_{NN}} = 2.76 \text{ TeV}$ and Au–Au collisions at $\sqrt{s_{NN}} = 200 \text{ GeV}$ measured by ALICE and STAR collaboration, respectively.

The observed p_T dependence of ρ_{00} for K^{*0} vector meson in heavy-ion collisions at both LHC and RHIC energies and for ϕ meson at LHC energy are qualitatively consistent with the prediction from the quark recombination model of polarized quarks^{3–5,38} which attributes the spin alignment to polarization of quarks in the presence of large initial angular momentum in non-central heavy-ion collisions and a subsequent hadronization by the process of recombination. However, ρ_{00} for ϕ mesons are larger than $1/3$ in mid-central Au–Au collisions at $\sqrt{s_{NN}} = 200 \text{ GeV}$.⁴⁴ The $\rho_{00} > 1/3$ for ϕ mesons can not be explained by naive quark re-

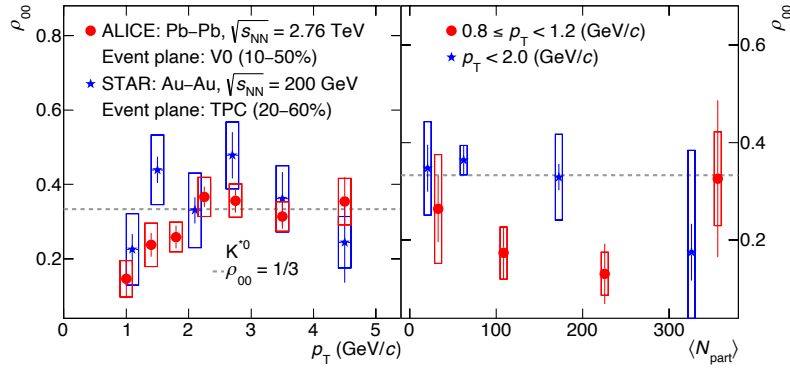


Fig. 11. Left panel: ρ_{00} vs. p_T for K^{*0} meson at $|y| < 0.5$ in mid-central Pb-Pb and Au-Au collisions at $\sqrt{s_{NN}} = 2.76$ TeV¹² and 200 GeV.¹³ The statistical and systematic uncertainties are shown as bars and boxes, respectively.

combination and fragmentation model³ but may come from the electric part of the ϕ meson field.³⁹ The centrality or $\langle N_{part} \rangle$ dependence of ρ_{00} is qualitatively consistent with the variation of initial angular momentum with impact parameter in heavy-ion collisions.² In recombination hadronization scenario of polarized quarks, the ρ_{00} of vector mesons are related to quark polarization as $\rho_{00} = \frac{1-P_q P_{\bar{q}}}{3+P_q P_{\bar{q}}}$ where

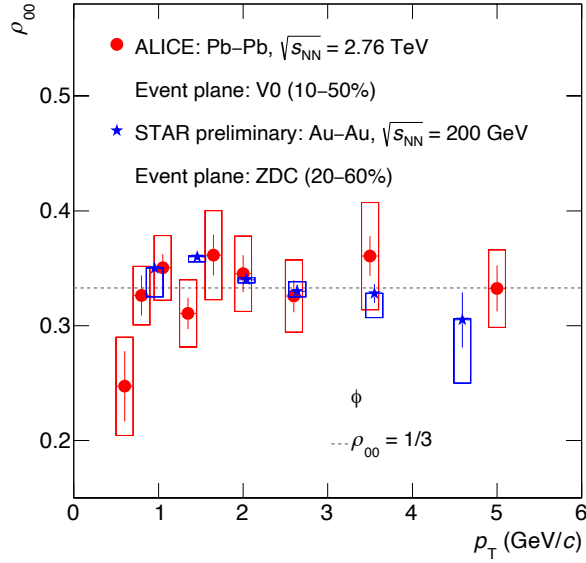


Fig. 12. Spin density matrix element ρ_{00} as a function of p_T for ϕ meson in mid-central Pb-Pb and Au-Au collisions at $\sqrt{s_{NN}} = 2.76$ TeV¹² and 200 GeV.⁴⁴ The statistical and systematic uncertainties are shown as bars and boxes, respectively.

P_q and $P_{\bar{q}}$ are the polarization of quark and anti-quark in presence of the initial angular momentum.³ Assuming the same quark polarization for light and strange quark and antiquark, measured ρ_{00} values can be used to estimate the order of quark polarization. Estimated quark polarization from quark recombination model is of the order of $O(0.1)$ ¹² and with the present uncertainties no significant energy dependence of quark polarization is observed.

Although the quark recombination model^{3-5,38} qualitatively describe the observed p_T dependence of ρ_{00} for K^{*0} vector meson in heavy-ion collisions at both LHC and RHIC energies and for ϕ meson at LHC energy but quantitatively the experimental results are surprisingly high compared to the model calculation in context of Λ polarization. While no quantitative theoretical calculation for vector meson spin alignment at LHC energies exists, the expected order of magnitude can

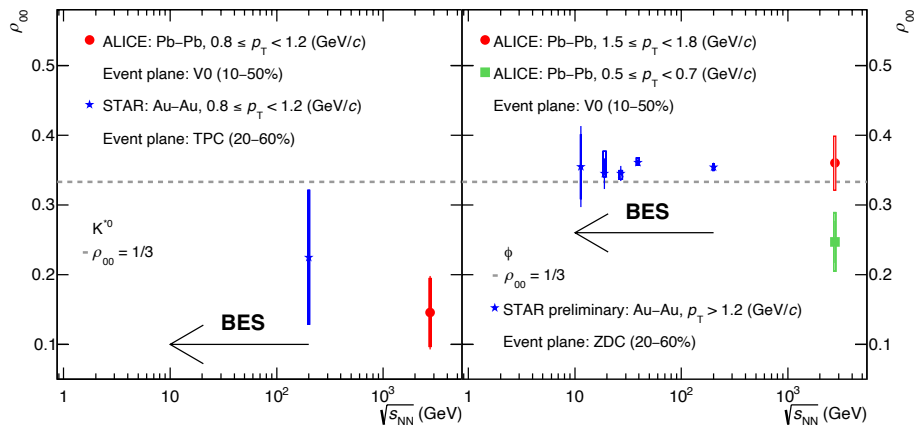


Fig. 13. Beam energy dependence of ρ_{00} for K^{*0} ^{12,13} and ϕ ^{12,44} vector mesons. Statistical and systematic uncertainties are shown by bars and boxes, respectively. BES represents the region to be explored by the beam energy scan program at RHIC.

be estimated and the measurements for vector mesons and hyperons can be related in a model dependent way. The polarization of Λ baryons (spin = 1/2) is about $O(1\%)$ at lower RHIC energies^{45,46} and decreases with energy to reach $O(0.1\%)$ at LHC energy.⁴⁷ In the quark recombination model, Λ polarization linearly depends on quark polarization³ (p_q), whereas ρ_{00} depends on the square of quark polarization.⁴ With these assumptions and taking the input of p_q from Λ polarization measurements at LHC energies,⁴⁷ one would expect spin alignment effect is very tiny and ρ_{00} is closed to 1/3. Therefore, the observed spin alignment of vector meson is surprisingly large in context of Λ polarization. Using a thermal and non-relativistic approach as discussed in,⁴⁰ vorticity (ω) and temperature (T) are related to hyperon polarization (P_Λ) and ρ_{00} as $P_\Lambda \simeq \frac{1}{4} \frac{\omega}{T}$ and $\rho_{00} \simeq \frac{1}{3} \left(1 - \frac{(\omega/T)^2}{3} \right)$, respectively. In this model framework, estimated spin alignment for vector mesons from Λ polarization measurements are also very tiny and $\rho_{00} \simeq 1/3$.

However, for spin 1/2 particles the angular distribution of the decay daughters is an odd function and hence depends on the sign of the angular momentum direction. For spin 1 particles the angular distribution of the decay daughters is an even function and only depends on the strength of the angular momentum not on the sign. Unlike vector mesons, hyperons also have a large decay contribution. The ρ_{00} value may also depend on the details of the transfer of the quark polarization to the hadrons during hadronization. In addition, re-scattering, regeneration, lifetime and mass of the hadron, and interaction of the hadron with the medium may also affect the magnitude of ρ_{00} . So far, the large magnitude of global spin alignment of K^{*0} and ϕ vector mesons compared to Λ polarization, observed in high energy heavy-ion collisions at RHIC and LHC energies cannot be explained by conventional effects such as vorticity field, electromagnetic field and recombination hadronization of polarized quarks. Recent theory development discussed in Ref.^{39,48} suggests a large positive deviation of ρ_{00} for ϕ mesons from 1/3 may come from the electric part of the ϕ meson field. Existence of ϕ meson field in high energy heavy-ion collisions may explain the significantly large spin alignment of ϕ vector mesons at RHIC energies. Vector meson field formalism is difficult to develop for K^{*0} meson because of the unequal masses of s and d quarks. Due to the unequal masses of constituent quarks, decoupling of the contribution from the vorticity, electric field, magnetic field and vector meson field is difficult for K^{*0} . In addition, due to the short lifetime of K^{*0} meson interaction of K^{*0} with the surrounding matter is much stronger than that of the ϕ meson and this may also affect the ρ_{00} values of K^{*0} .⁵⁰ Recent study in Ref.⁴⁹ shows that the deviation of ρ_{00} from 1/3 may also come from the local spin alignment of vector mesons. In this model framework, the large negative deviation of ρ_{00} from 1/3 ($\rho_{00} < 1/3$) is not solely coming from the global spin alignment but have also contribution from the local polarization of quarks and anti-quarks which are locally polarized due to the anisotropic expansion of the medium. However, the contribution from the local quark polarization in ρ_{00} is yet not constrained from the experiments as it requires the measurements for off

diagonal spin density matrix elements. Till now, no quantitative theory explanation for the measured spin alignment of vector meson at RHIC and LHC energies exists. Therefore these measurements will trigger further theoretical works to understand the results.

The measured Λ polarization value at RHIC^{45,46} and LHC⁴⁷ energies are found to be decreases with $\sqrt{s_{NN}}$. In quark model, non-relativistic hydrodynamics and ϕ meson field approach, estimated spin alignment of vector mesons from Λ polarization measurements reduces with $\sqrt{s_{NN}}$. However, within the present statistical uncertainties no such energy dependence of vector meson spin alignment is observed, as shown in Fig. 13. In future, high statistics BES II data at RHIC energies and in Pb–Pb collisions at 5.02 TeV data at LHC will help to look at the $\sqrt{s_{NN}}$ dependence of vector meson spin alignment with precise measurements.

7. Summary and outlook

The spin alignment measurements have been studied in e^+e^- and hadron collisions for decades to understand the vector meson production mechanism. Measurements of spin density matrix element ρ_{00} with respect to the helicity frame in e^+e^- collisions^{25–27} shows an evidence of spin alignment of vector mesons produced in high x_p region. The ρ_{00} values are found to be larger than the 1/3 for K^{*0} , ϕ and ρ mesons. This observation suggests that the fragmentation of an unpolarized quark led to vector meson with a larger probability at the helicity zero state. This observations are consistent with the QCD based model¹⁶ in which vector meson production is arising from the helicity conserving process $q \rightarrow qV$. Other QCD models^{19–21} based on the equal distribution of hadron energy in constituent quarks also prefer the production of vector meson with helicity state zero. On the other hand measurements of off diagonal spin density matrix elements are consistent with zero ruling out coherence models^{22–24} which predicted non zero off diagonal elements. The spin alignment measurements for K^{*0} and K^{*+} vector mesons have also been studied in kp and nC interaction^{28–32} with respect to the direction perpendicular to the production plane. In these experiments, the measured ρ_{00} values are found to be larger than the 1/3 and can be explained by a parton recombination model³⁴ which attributes to the spin alignment of vector mesons via Thomas precession of the quark's spins in the recombination process of hadronization. Measurements for spin density matrix element ρ_{00} have been further extended in pp collisions at $\sqrt{s} = 200$ GeV³⁵ and 13 TeV¹² with respect to the production plane. Measurements are found to be consistent with 1/3 in measured p_T region ($p_T < 5$ GeV/ c). In future, using high statistics pp collisions data at RHIC and LHC energies, these measurements can be carried out at high x_p region where recent theory study in Ref.³⁶ predicts a significant spin alignment for vector mesons.

Given the importance of spin-orbit interactions in several fields of physics, it is imperative to look for its possible effect on particles with spin in a system with high orbital angular momentum. Knowing the presence of the large angular momen-

tum created in non-central heavy-ion collisions, it is important to study the spin alignment of vector mesons to understand the spin orbital angular momentum interaction in QCD matter. Recent measurements of ρ_{00} for K^{*0} and ϕ vector mesons in Pb–Pb collisions at the LHC and in Au–Au collisions at the RHIC reported significant spin alignment. The ALICE experiment¹² has observed a significant spin alignment effect at a level of 3σ for K^{*0} and 2σ for ϕ in mid-central Pb–Pb collisions at $\sqrt{s_{\text{NN}}} = 2.76$ TeV due to the spin orbital angular momentum interaction. The spin density matrix element ρ_{00} is found to be lower than $1/3$ at $p_{\text{T}} < 2$ GeV/ c , whereas at high p_{T} the measurements are consistent with $1/3$. In order to validate the measurements, various control measurements such as measurements of ρ_{00} for vector mesons with respect to the random event plane, measurements of ρ_{00} for K_{S}^0 in mid-central heavy-ion collisions, and spin alignment measurements of vector mesons in pp collisions are carried out. In all control measurements measured ρ_{00} values are consistent with $1/3$. The observed p_{T} dependence of measured ρ_{00} values for vector mesons in mid-central Pb–Pb collisions can be attributed as a presence of a large initial angular momentum in non-central heavy-ion collisions, which leads to quark polarization via spin-orbit coupling, subsequently transferred to hadronic degrees of freedom by hadronization via recombination. However, the preliminary spin alignment measurements for ϕ meson at RHIC energies show $\rho_{00} > 1/3$ at intermediate p_{T} . The $\rho_{00} > 1/3$ for ϕ mesons can not be explained by naive quark recombination and fragmentation model but can be explained due to the presence of ϕ meson field in heavy-ion collisions. The spin alignment effect of vector mesons is maximum in mid-central Pb–Pb collisions, whereas in central and peripheral collisions the ρ_{00} values are consistent with $1/3$. The centrality dependence of spin alignment effect of vector meson is consistent with the impact parameter dependence of initial angular momentum. Although a significant spin alignment effect of vector mesons have been observed but the measured spin alignment of vector mesons is surprisingly large compared to the polarization measured for Λ hyperons. Possible reason behind the large difference between Λ polarization and vector meson spin alignment may include the transfer of the quark polarization to the hadrons (baryon vs. meson), details of the hadronization mechanism (recombination vs. fragmentation), re-scattering, regeneration, and possibly the lifetime and mass of the relevant hadron. Moreover, the vector mesons are predominantly directly produced whereas the hyperons have large contributions from resonance decays. So far, there are no quantitative theory explanation for the large ρ_{00} values of K^{*0} and ϕ vector mesons observed at RHIC and LHC energies and these measurements will trigger further theoretical works in order to study which effects could make such a huge difference between Λ and vector meson polarization. However, recent theory developments which incorporate vector meson field and local polarization may explain the large spin alignment of vector mesons.

In future, high statistics data at the RHIC and LHC energies will provide precise measurements and can be useful to understand the beam energy dependence of ρ_{00} . High statistics data may allow the possibility of assessing the effect of initial

magnetic field produced in heavy-ion collisions by measuring the difference in the spin alignment of $K^{*\pm}$ and K^{*0} as the magnetic moment of $K^{*\pm}$ is ~ 7 times larger than the K^{*0} . Measurements of the off diagonal spin density matrix elements and azimuthal angle (vector meson azimuthal angle with respect to the reaction plane angle) dependency of ρ_{00} can be used to disentangle the local spin alignment from the global spin alignment. In addition, extension of spin alignment study at high p_T in pp collisions will be useful to constrain the spin dependent fragmentation function.

Acknowledgments

B.M. was supported in part J C Bose Fellowship from Department of Science of Technology, Government of India and Research in Basic Sciences project from Department of Atomic Energy, Government of India. SS is supported by the Strategic Priority Research Program of Chinese Academy of Sciences (Grant XDB34000000).

References

1. P. Braun-Munzinger and J. Stachel, *Nature* 448, 302 (2007).
2. F. Becattini et al., *Phys. Rev. C* 77, 024906 (2008).
3. Z.-T. Liang et al., *Phys. Rev. Lett.* 94, 102301 (2005).
4. Z.-T. Liang et al., *Phys. Lett. B* 629, 20 (2005).
5. Z.-T. Liang, *J. Phys. G* 34, S323 (2007).
6. H. Li, L. G. Pang, Q. Wang and X. L. Xia, *Phys. Rev. C* 96, 054908 (2017).
7. W. Florkowski, B. Friman, A. Jaiswal and E. Speranza, *Phys. Rev. C* 97, 041901 (2018).
8. F. Becattini and I. Karpenko, *Phys. Rev. Lett.* 120 012302 (2018).
9. N. Weickgenannt, X. L. Sheng, E. Speranza, Q. Wang and D. H. Rischke, *Phys. Rev. D* 100, 056018 (2019).
10. K. Schilling et al., *Nucl. Phys. B* 15, 397 (1970).
11. M. E. Rose, *Elementary theory of angular momentum* [John Wiley & Sons, Inc.], 1957.
12. S. Acharya et al. (ALICE Collaboration), *Phys. Rev. Lett.* 125, 012301 (2020).
13. B. I. Abelev et al. (STAR Collaboration), *Phys. Rev. C* 77, 061902 (2008).
14. A. H. Tang et al., *Phys. Rev. C* 98, 044907 (2018).
15. R. Singh, *Nucl. Phys. A* 982, 515 (2019).
16. J. F. Donoghue, *Phys. Rev. D* 19, 2806 (1979).
17. I. I. Y. Bigi, *Nuovo Cimento A* 41, 581 (1977).
18. J. E. Augustin et al., *Nucl. Phys. B* 162, 341 (1980).
19. G. R. Farrar et al., *Phys. Rev. Lett.* 35, 1416 (1975).
20. A.I. Vainstein et al., *Phys. Lett. B* 72 (1978) 368.
21. R. Suaya et al., SLAC-PUB 2190 (1978).
22. M. Anselmino et al., *Z. Phys. C* 29, 135 (1985).
23. A. Anselm et al., *J. Exp. Th. Phys. Lett.* 60, 496 (1994).
24. M. Anselmino et al., Preprint DFTT 25/97, INFNCA-TH9707 (1997).
25. K. Ackerstaff et al. (OPAL Collaboration), *Phys. Lett. B* 412, 210 (1997).
26. K. Ackerstaff et al. (OPAL Collaboration), *Z. Phys. C* 74, 437 (1997).
27. P. Abreu et al. (DELPHI Collaboration), *Phys. Lett. B* 406, 271 (1997).
28. P. Chliapnikov et al., *Nucl. Phys B* 37, 336 (1972).
29. I. V. Ajinenko et al. (French-Soviet and CERN-Soviet Collaborations), *Z. Phys. C* 5, 177 (1980).

30. M. Barth et al. (Brussels-Genoa-Mons-Nijmegen-Serpukhov-CERN Collaboration), Nucl. Phys. B 223, 296 (1983).
31. K. Paler et al., Nucl. Phys. B 96, 1 (1975).
32. Yu. Arestov et al. (French-Soviet and CERN-Soviet Collaborations), Z. Phys. C 6, 101 (1980).
33. A. N. Alev et al. (EXCHARM Collaboration), Phys. Lett. B 485, 334 (2000).
34. A. Ayala et al., Phys Lett. B 682, 408 (2010).
35. B. I. Abelev et al. (STAR Collaboration), Phys. Rev. C 77, 061902 (2008).
36. K. Chen et al., Phys. Rev. D 102, 034001 (2020).
37. S. A. Voloshin, arXiv:0410089[nucl-th].
38. Y. -G. Yang et al., Phys. Rev. C 97, 034917 (2018).
39. X. -L. Sheng et al., Phys. Rev. D 101, 096005 (2020).
40. F. Becattini et al., Phys. Rev. C 95, 054902 (2017).
41. T. Sjöstrand et al., Comput. Phys. Commun. 191, 159 (2015).
42. B. B. Abelev et al. [ALICE Collaboration], JHEP 06, 190 (2015).
43. A. H. Tang et al., Phys. Rev. C 98, 044907 (2018).
44. C. Zhou [STAR collaboration], Nucl. Phys. A 982, 559 (2019).
45. L. Adamczyk et al. [STAR Collaboration], Nature 548, 62 (2017).
46. J. Adam et al. [STAR Collaboration], Phys. Rev. C 98, 014910 (2018).
47. S. Acharya et al. [ALICE Collaboration], arXiv:1909.01281[nucl-ex].
48. X. -L. Sheng et al., Phys. Rev. D 102, 056013 (2020).
49. X.-L. Xia et al., arxiv:2010.01474 [nucl-th].
50. D. Shen et al., Chin. Phys. C 45, 054002 (2021)